JCIM JOURNAL OF CHEMICAL INFORMATION AND MODELING

pubs.acs.org/jcim

Application Note

Hotspots API: A Python Package for the Detection of Small Molecule Binding Hotspots and Application to Structure-Based Drug Design

Peter R. Curran,*[,■] Chris J. Radoux,[■] Mihaela D. Smilova, Richard A. Sykes, Alicia P. Higueruelo, Anthony R. Bradley, Brian D. Marsden, David R. Spring, Tom L. Blundell, Andrew R. Leach, William R. Pitt, and Jason C. Cole*

Cite This: *J. Chem. Inf. Model.* 2020, 60, 1911−1916

Read Online

ACCESS | Metrics & More | Article Recommendations

ABSTRACT: Methods that survey protein surfaces for binding hotspots can help to evaluate target tractability and guide exploration of potential ligand binding regions. Fragment Hotspot Maps builds upon interaction data mined from the CSD (Cambridge Structural Database) and exploits the idea of identifying hotspots using small chemical fragments, which is now widely used to design new drug leads. Prior to this publication, Fragment Hotspot Maps was only publicly available through a web application. To increase the accessibility of this algorithm we present the Hotspots API (application programming interface), a toolkit that offers programmatic access to the core Fragment Hotspot Maps algorithm, thereby facilitating the interpretation and application of the analysis. To demonstrate the package's utility, we present a workflow which automatically derives protein hydrogen-bond constraints for molecular docking with GOLD. The Hotspots API is available from https://github.com/prcurran/hotspots under the MIT license and is dependent upon the commercial CSD Python API.

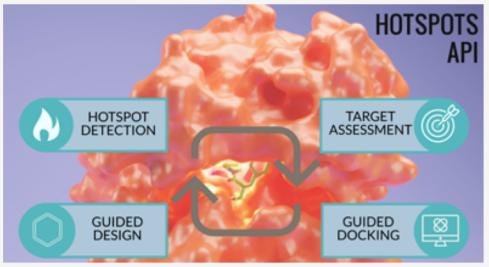

■ INTRODUCTION

In the context of protein−ligand interactions, the term "hotspot" describes a region within a pocket that contributes a disproportionately large amount to the overall binding energy.[1] We previously described a hotspot as "the minimum binding site that will bind a fragment, maintaining the fragment binding position once it has been elaborated".[2] Fragment experiments can yield useful information about the tractability of a target[1] or be used to guide structure-based drug design.[3] It follows that the presence of a computationally determined hotspot can be used in the same way.[4]

There have been many computational approaches to map potential protein−ligand interactions within pockets.[5−7] Fragment Hotspot Maps,[2] and other more recent methods,[8−11] go further by differentiating between the available interactions, highlighting the most preferential.

Prior to this communication, the Fragment Hotspot Maps method was only publicly available through a web application (http://fragment-hotspot-maps.ccdc.cam.ac.uk). While this provided easy access to the method, it allowed only for visual inspection of the results, limiting how the information could be used, particularly for large scale applications or as part of existing structure-based drug design (SBDD) workflows.

Herein, we present the Hotspots API. For the general user, this provides direct access to the calculation, enabling analysis of confidential structures and facilitating the integration of results with other SBDD methods. For these users, we provide example workflows as "cookbook" examples in the API documentation which include tractability assessment, pharmacophore searching, and docking. As an example, we discuss how to use Fragment Hotspot Maps to automatically generate GOLD[12] docking constraints. For developers, the open source code base offers a platform for collaboration and has enabled researchers from several institutions to start projects to create new features and applications.

Fragment Hotspot Maps Background. *Isostar and SuperStar.* The Fragment Hotspot Maps approach builds on the previous work of IsoStar[13] and SuperStar,[6] released in 1999. In IsoStar, patterns of interactions are constructed by searching for all structures containing a given pair of predefined functional groups, which are then assessed to search for nonbonded contacts between the two groups (a central group and a contact group). Each 3D hit is transformed such that the central groups are superimposed. This leads to a scatterplot of contact group atomic positions around the central group (Figure 1a). As detailed in the original SuperStar paper,[6] scatterplots can be converted into grids by calculating

Received: October 28, 2019
Published: March 24, 2020

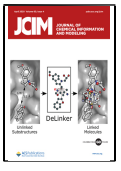

https://dx.doi.org/10.1021/acs.jcim.9b00996
J. Chem. Inf. Model. 2020, 60, 1911−1916

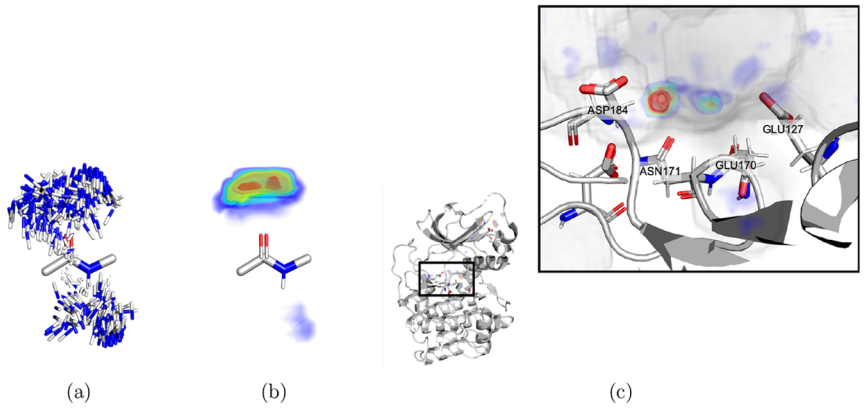

Figure 1. (a) Example IsoStar scatterplot (central group: peptide, contact group: uncharged NH nitrogen). 1815 CSD entries are displayed with their central group superimposed to reveal the spatial distribution of interacting uncharged NH nitrogens atoms. All atoms not in the central or contact groups are hidden. (b) Scaled density of uncharged NH nitrogen atoms around the peptide fragment (blue = less dense, red = more dense). (c) SuperStar grid for Uncharged NH nitrogen atomic probe calculated for AKT1 (PDB: 4c33). Several residues are labeled to highlight the central-contact pairings.

the observed density of a given probe atom at all grid points. The grid can then be scaled to an absolute level: An "average density" expected for a given central group, contact group pair across all entries where a contact could occur is calculated. This is then used to divide all the observed densities at a given grid point. Plots are generated for 320 predefined central groups contacting 26 contact groups, covering a wide variety of chemical fragments in the CSD and an example scatterplot and propensity grid are given in Figure 1a and b.

SuperStar takes the appropriate central group distributions in IsoStar for a given contact group and superimposes them onto protein residues to generate a composite distribution that covers all the solvent exposed regions in a protein (or protein binding site) for that contact group. Each composite distribution can be transformed into a contour surface using counts of atoms within a given grid cube around the central group. This can in turn be scaled using the methods outlined above. The outcome is a scaled map that represents the relative likelihood of an interaction by a given contact group at all exposed locations in a protein. An example SuperStar map, calculated for AKT1 (PDB: 4c33), is given in Figure 1.

Fragment Hotspot Maps Method. Several studies[14−16] have described hotspot environments as enclosed, hydrophobic regions that are capable of hydrogen bonding. Principally, Fragment Hotspot Maps seeks to prioritize SuperStar's cavity annotations that are located in these environments. To do this, grid-based atomic propensity scores are generated by SuperStar for apolar ("Aromatic CH Carbon atom"), donor ("Uncharged NH Nitrogen atom"), and acceptor ("Carbonyl Oxygen atom") atomic probes. In order to introduce enclosure, these interaction maps are then weighted by buriedness, so that more buried sites are favored over less buried sites.[17]

Originally, the LIGSITE[18] algorithm was used, however it was found that some SuperStar grid points close to the pocket edge were incorrectly classified by LIGSITE as "clashing", meaning that key intermolecular interaction sites were not being detected. Therefore, access to an alternative pocket detection method, Ghecom[19] is provided. To maintain the same scoring regime as LIGSITE, the Ghecom scores are reversed and scaled between 1 and 7 (1 less buried, 7 most buried).

The weighted interaction grids, are then sampled with pseudomolecular probes that reflect the nature of hotspot environments. Figure 2, depicts the default probes. In the latest release, additional probes are available including different sized, shaped and charged groups, but these are currently unvalidated.

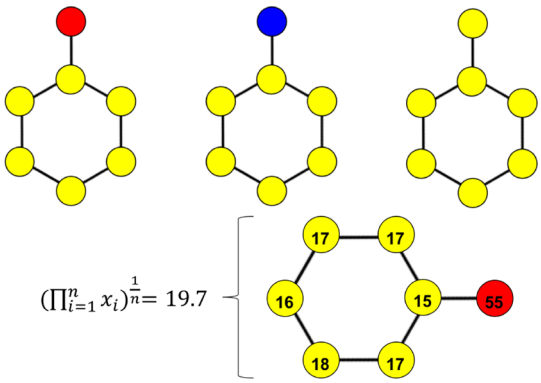

Figure 2. Three probes used to generate acceptor (left), donor (middle), and apolar (right) hotspot maps. Red atoms are treated as hydrogen bond acceptors, blue atoms, as hydrogen bond donors, and yellow, as apolar. At the bottom, an example calculation is given to show how the probe score is derived from the geometric mean of the atomic scores.

The polar probes contain a polar atom in the substituted position. The weighted interaction grids are sampled by their corresponding probe. Probes are translated to all grid points above a threshold (default = 15) and are randomly rotated around the center of the "substituted" atom. Sampling optimizations have allowed the number of rotational samples to increase from 200 to 3000 rotations which leads to more consistent map scores. For each pose, the probe atom scores are read from their corresponding grids using linear interpolation.

The probe scores are determined by calculating the geometric mean of the atom scores, as shown in Figure 2. The geometric mean ensures all poses that clash with the protein are eliminated. Once scored, the sampled probes scores are assigned to an output grid. For polar probes, the probe

https://dx.doi.org/10.1021/acs.jcim.9b00996
J. Chem. Inf. Model. 2020, 60, 1911−1916

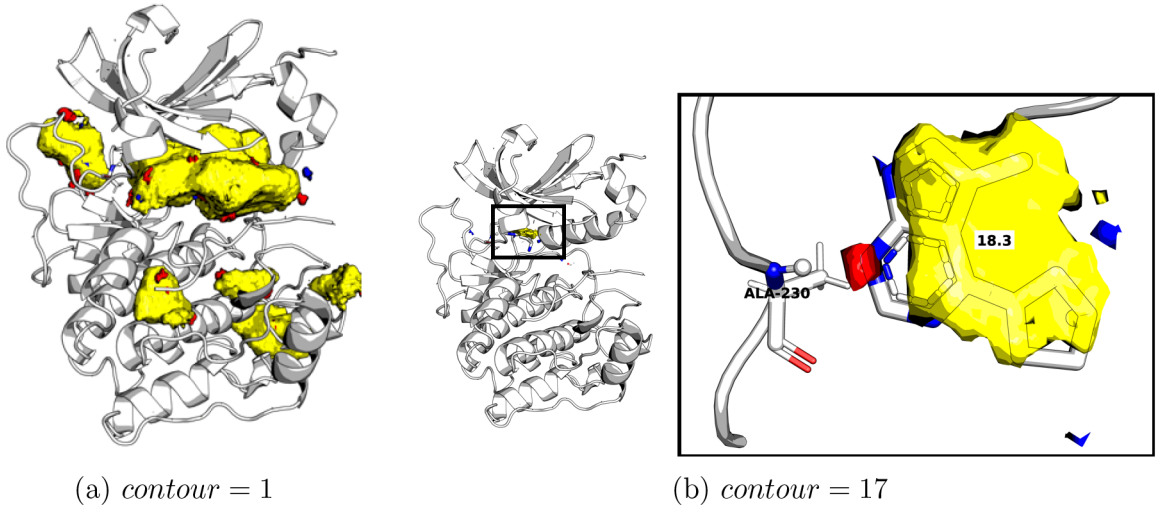

Figure 3. Fragment Hotspot Map calculated for AKT1 (PDB Code: 3cqw), showing apolar (yellow), donor (blue), and acceptor (red) maps. Figure 3b shows the key backbone NH of ALA230 displayed in ball and sticks and a bound fragment aligned from a second protein structure (PDB Code: 3mv5).

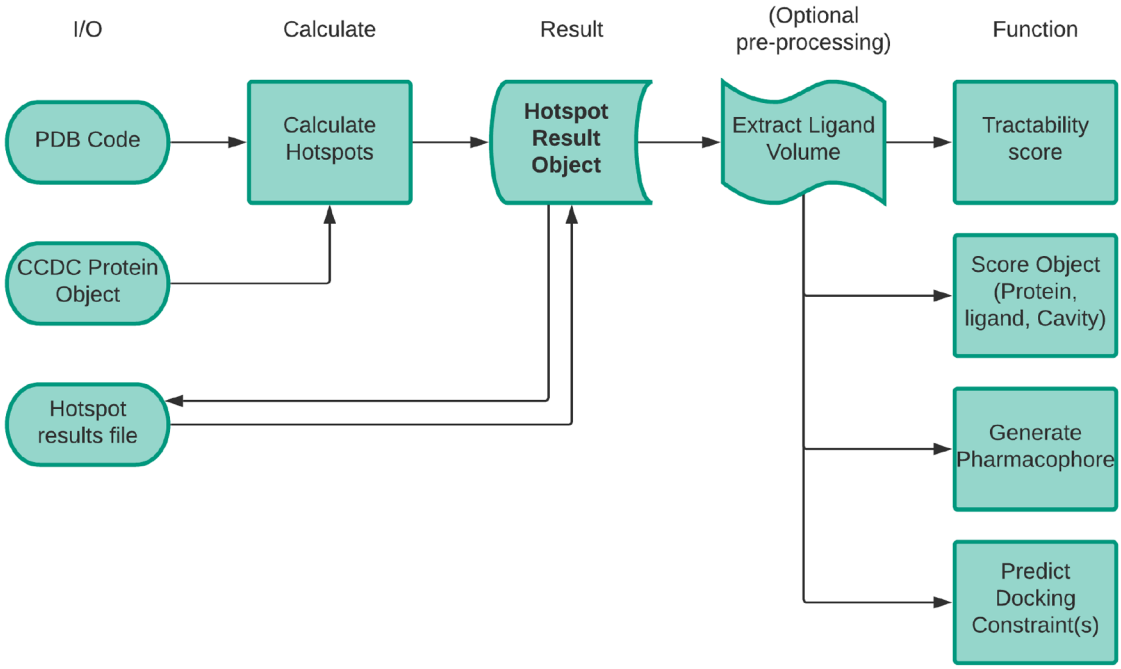

Figure 4. Overview of the key functionality of the Hotspots API.

score is assigned only to the polar atom position in the corresponding output grid, while for the apolar probes, the probe score is assigned to all atom positions. The probe score is only assigned if it is greater than the existing grid point score.

Fragment Hotspot Maps Output. Figure 3 shows an example Fragment Hotspot Maps output for AKT1 (PDB: 3cqw) contoured at score = 1 (Figure 3a) and score = 17 (Figure 3b). This demonstrates that, while all pockets are sampled, the very highest scoring regions correspond to the hotspot.

Knowledge of these key interactions are normally determined through structure−activity relationships (SARs) and other experimental data. Once highlighted, these key interactions can be utilized by SBDD methods to improve performance.[20] Predicting these key interactions *a priori* allows the user to take advantage of this improved performance, starting from the structure alone.

APPLICATION EXAMPLES

The Hotspots API has been applied in several different domains, as summarized in Figure 4. The API has been used to assess target tractability and to generate pharamcophores for a give target structure. Cookbook examples are provided in the API documentation (https://github.com/prcurran/hotspots/blob/master/documentation.pdf) that demonstrate these use cases. In addition, the API can be used for automating the setting of docking constraints. We elaborate on this example further here.

Case Study: Automatically Generated Docking Constraints. For this example, we use AKT1 (PDB: 3cqw), a

https://dx.doi.org/10.1021/acs.jcim.9b00996
J. Chem. Inf. Model. 2020, 60, 1911−1916

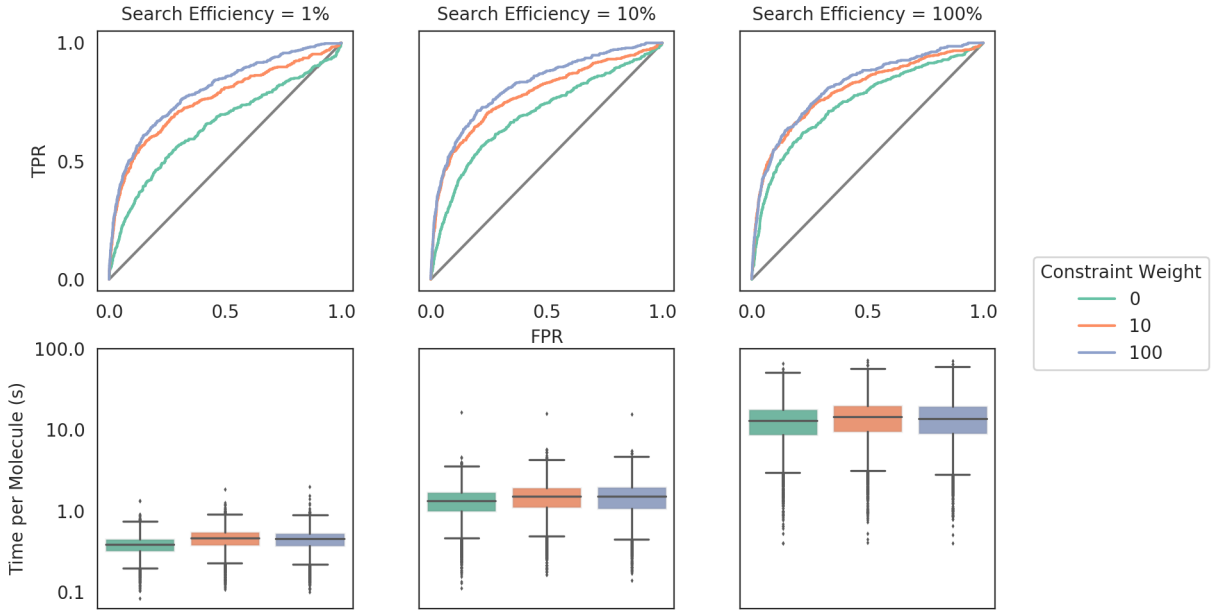

Figure 5. (top) Receiver operating characteristic (ROC) curves and (bottom) box plots showing time per molecule for comparing constraint weights of 0 (green), 10 (orange), and 100 (blue) for search efficiencies of 1% (left), 10% (middle), and 100%.

Table 1. Summary of the Nine Docking Calculations Performed[a]

GOLD settings		enrichment statistics					
search efficiency	weight	AUC	$EF_{1\%}$	$EF_{5\%}$	$EF_{10\%}$	$BEDROC_{\alpha=16}$	$BEDROC_{\alpha=8}$
1	0	0.65	5.2	3.74	2.98	0.23	0.32
1	10	0.76	10.64	6.95	4.7	0.38	0.48
1	100	0.8	12.53	7.33	5.04	0.41	0.51
10	0	0.7	5.2	4.35	3.4	0.26	0.37
10	10	0.78	11.35	7.61	5.22	0.42	0.51
10	100	0.82	13	7.85	5.39	0.44	0.54
100	0	0.74	6.15	5.82	4.33	0.33	0.43
100	10	0.8	11.35	7.8	5.32	0.42	0.52
100	100	0.82	12.77	7.85	5.27	0.42	0.52

[a]For each combination of search efficiency and constraint weight the rank statistics are provided to demonstrate effect on virtual screening performance. Area under the ROC curve (AUC) is a metric to evaluate performance across the whole dataset whereas enrichment factor and Boltzmann-enhanced discrimination of ROC[27] (BEDROC) focus upon early enrichment making them highly relevant to virtual screening tasks.

member of the DUD-e diverse set, and screen against the corresponding DUD-e ligands (423 "actives" and 16576 "decoys").[21]

Modeling protein−ligand interactions through molecular docking is a routine technique for pose prediction and virtual screening.[22] Prior knowledge of important interactions with the target protein can enhance docking performance using protein hydrogen-bonding constraints.[23] Constraints can be used to reduce the search space to be explored or to filter solutions thereby impacting both speed and accuracy. When working on a novel target or pocket, it may not be obvious which interactions should be prioritized via constraints. Roca et al.[24] performed docking with Glide[25] on an allosteric site of AChE, identified by Fragment Hotspot Maps. Visual inspection of the maps allowed them to filter molecules making key interactions. Subsequent testing found some molecules to be functionally active inhibitors, and the docking and hotspot analysis suggests this is through allosteric binding. Furthermore, previous work[26] has suggested Fragment Hotspot results can improve enrichment rates in molecular docking and that the weighting of the constraints can, in turn, effect the level of improvement.

Workflow. It is possible to setup and run GOLD docking calculations using the CSD Python API, including the addition of constraints. Several constraint types are available, but here we focus on the protein hydrogen bond constraint, which applies a penalty to any ligand poses that do not hydrogen bond to the chosen protein atom.

Nine GOLD docking calculations were run with all the combinations of search efficiencies (1, 10, and 100) and constraint weights (0, 10, 100). A single protein hydrogen bond constraint is determined automatically using the following workflow:

- Use CSD Python API to setup GOLD, with all other settings set to default (section 3.3, Hotspot API documentation).
- Calculate Fragment Hotspot Maps for the docking receptor.
- Score protein atoms using their complementary map. Using the backbone NH shown in Figure 3b as an

https://dx.doi.org/10.1021/acs.jcim.9b00996
J. Chem. Inf. Model. 2020, 60, 1911−1916

example, the score is read from the red acceptor map using the vector of the NH bond.

- Set a protein hydrogen bond constraint on the highest scoring polar atom: in this case, the backbone NH of ALA230 at the kinase hinge.
- Run GOLD dockings.

Results. As can be seen from Figure 5 and Table 1, applying H-bond constraints based on hotspot maps improves the retrieval performance for this example. The most significant effect is on retrieval speed. GOLD can be run using different search efficiencies which control the degree of sampling in the genetic algorithm. By using automated constraints, one can outperform 100% search efficiency results in 1% search efficiency settings; a speed improvement of more than an order of magnitude. While this work showcases this use case, we will undertake further work in future to evaluate the benefit more generally across a wider range of targets.

CONCLUSION

The Hotspots API is a Python package that extends functionality offered by the CSD Python API to enable access to the Fragment Hotspot Maps algorithm and provides support for applying the results. The API enables users to start with no prior knowledge of their biological system and identify critical intermolecular interactions. We demonstrate how the results can be automatically used in molecular docking with GOLD. Cookbook examples (tractability and pharmacophore generation) are also available for other applications in the API documentation. (https://github.com/prcurran/hotspots/blob/master/documentation.pdf). This functionality is available through one package and can be deployed with minimal code required from the user and therefore offers a powerful resource for early drug design.

Furthermore, this package provides the building blocks and framework for collaborative approaches to tackle more complex problems in structure-based design such as predicting selectivity profiles and guiding fragment elaboration.

AUTHOR INFORMATION

Corresponding Authors

Peter R. Curran − *The Cambridge Crystallographic Data Centre (CCDC), Cambridge CB2 1EZ, U.K.; Department of Chemistry, University of Cambridge, Cambridge CB2 1EW, U.K.*; Email: pcurran@ccdc.cam.ac.uk

Jason C. Cole − *The Cambridge Crystallographic Data Centre (CCDC), Cambridge CB2 1EZ, U.K.*; orcid.org/0000-0002-0291-6317; Email: cole@ccdc.cam.ac.uk

Authors

Chris J. Radoux − *Exscientia Ltd., Oxford OX1 3LD, U.K.*

Mihaela D. Smilova − *Structural Genomic Consortium (SGC), Nuffield Department of Medicine, University of Oxford, Oxford OX3 7DQ, U.K.*

Richard A. Sykes − *The Cambridge Crystallographic Data Centre (CCDC), Cambridge CB2 1EZ, U.K.*

Alicia P. Higueruelo − *The Cambridge Crystallographic Data Centre (CCDC), Cambridge CB2 1EZ, U.K.*

Anthony R. Bradley − *Exscientia Ltd., Oxford OX1 3LD, U.K.*

Brian D. Marsden − *Structural Genomic Consortium (SGC), Nuffield Department of Medicine and Kennedy Institute of Rheumatology, NDORMS, University of Oxford, Oxford OX3 7DQ, U.K.*

David R. Spring − *Department of Chemistry, University of Cambridge, Cambridge CB2 1EW, U.K.*; orcid.org/0000-0001-7355-2824

Tom L. Blundell − *Department of Biochemistry, University of Cambridge, Cambridge CB2 1GA, U.K.*

Andrew R. Leach − *Chemogenomics Team, European Bioinformatics Institute (EMBL-EBI), Cambridge CB10 1SD, U.K.*

William R. Pitt − *UCB Pharma, Berkshire SL1 3WE, U.K.*; orcid.org/0000-0001-8164-4550

Complete contact information is available at: https://pubs.acs.org/10.1021/acs.jcim.9b00996

Author Contributions

■P.R.C. and C.J.R. contributed equally.

Funding

P.R.C was funded by the Biotechnology and Biological Sciences Research Council and UCB (BB/P50466X/1). C.J.R. was funded by Open Targets. M.D.S. was supported by funding from the Engineering and Physical Sciences Research Council (EPSRC), the Medical Research Council (MRC), Exscientia, and the CCDC [grant number EP/L016044/1]. B.D.M. was supported by funding from the SGC and The Kennedy Trust for Rheumatology Research. The SGC is a registered charity (number 1097737) that receives funds from AbbVie, Bayer Pharma AG, Boehringer Ingelheim, Canada Foundation for Innovation, Eshelman Institute for Innovation, Genome Canada, Innovative Medicines Initiative (EU/EFPIA) [ULTRA-DD grant no. 115766], Janssen, Merck KGaA Darmstadt Germany, MSD, Novartis Pharma AG, Ontario Ministry of Economic Development and Innovation, Pfizer, São Paulo Research Foundation−FAPESP, Takeda, and Wellcome [106169/ZZ14/Z]. R.A.S. and D.R.S. acknowledge support from the Engineering and Physical Sciences Research Council (EP/P020291/1) and Royal Society (Wolfson Research Merit Award).

Notes

The authors declare the following competing financial interest(s): J.C.C. works for the CCDC, the creators of the underlying software (the CSD System) that is used by this library to generate the maps.

This Python 3 package is available for download from https://github.com/prcurran/hotspots under an open-source license. The software depends on the CSD Python API which is part of CCDC's CSD-Discovery package which is available under a commercial license. The software can be evaluated by arrangement with CCDC. Other dependencies (open-source) and versions are available in the repository, and we recommend installing within a conda environment created from the environment.yaml file provided in the repository.

ACKNOWLEDGMENTS

The authors thank the CCDC Discovery team for their helpful discussions and comments.

REFERENCES

(1) Hajduk, P. J.; Huth, J. R.; Tse, C. Predicting protein druggability. *Drug Discovery Today* **2005**, *10*, 1675−82.

(2) Radoux, C. J.; Olsson, T. S. G.; Pitt, W. R.; Groom, C. R.; Blundell, T. L. Identifying Interactions that Determine Fragment Binding at Protein Hotspots. *J. Med. Chem.* **2016**, *59*, 4314−25.

(3) Kamada, Y.; Sakai, N.; Sogabe, S.; Ida, K.; Oki, H.; Sakamoto, K.; Lane, W.; Snell, G.; Iida, M.; Imaeda, Y.; Sakamoto, J.; Matsui, J. Discovery of a B-Cell Lymphoma 6 Protein-Protein Interaction Inhibitor by a Biophysics-Driven Fragment-Based Approach. *J. Med. Chem.* **2017**, *60*, 4358−4368.
(4) Kozakov, D.; Hall, D. R.; Napoleon, R. L.; Yueh, C.; Whitty, A.; Vajda, S. New Frontiers in Druggability. *J. Med. Chem.* **2015**, *58*, 9063−9088.
(5) Goodford, P. J. A computational procedure for determining energetically favorable binding sites on biologically important macromolecules. *J. Med. Chem.* **1985**, *28*, 849−857.
(6) Verdonk, M. L.; Cole, J. C.; Taylor, R. SuperStar: A knowledge-based approach for identifying interaction sites in proteins. *J. Mol. Biol.* **1999**, *289*, 1093−1108.
(7) Caflisch, A.; Miranker, A.; Karplus, M. Multiple copy simultaneous search and construction of ligands in binding sites: application to inhibitors of HIV-1 aspartic proteinase. *J. Med. Chem.* **1993**, *36*, 2142−67.
(8) Böhm, H. J. The computer program LUDI: a new method for the de novo design of enzyme inhibitors. *J. Comput.-Aided Mol. Des.* **1992**, *6*, 61−78.
(9) Hall, D. R.; Ngan, C. H.; Zerbe, B. S.; Kozakov, D.; Vajda, S. Hot spot analysis for driving the development of hits into leads in fragment-based drug discovery. *J. Chem. Inf. Model.* **2012**, *52*, 199−209.
(10) Alvarez-Garcia, D.; Barril, X. Molecular Simulations with Solvent Competition Quantify Water Displaceability and Provide Accurate Interaction Maps of Protein Binding Sites. *J. Med. Chem.* **2014**, *57*, 8530−8539.
(11) Rathi, P. C.; Ludlow, R. F.; Hall, R. J.; Murray, C. W.; Mortenson, P. N.; Verdonk, M. L. Predicting "Hot" and "Warm" Spots for Fragment Binding. *J. Med. Chem.* **2017**, *60*, 4036−4046.
(12) Jones, G.; Willett, P.; Glen, R. C.; Leach, A. R.; Taylor, R. Development and validation of a genetic algorithm for flexible docking. *J. Mol. Biol.* **1997**, *267*, 727−48.
(13) Bruno, I. J.; Cole, J. C.; Lommerse, J. P.; Rowland, R. S.; Taylor, R.; Verdonk, M. L. IsoStar: a library of information about nonbonded interactions. *J. Comput.-Aided Mol. Des.* **1997**, *11*, 525−37.
(14) Young, T.; Abel, R.; Kim, B.; Berne, B. J.; Friesner, R. A. Motifs for molecular recognition exploiting hydrophobic enclosure in protein-ligand binding. *Proc. Natl. Acad. Sci. U. S. A.* **2007**, *104*, 808−813.
(15) Ichihara, O.; Shimada, Y.; Yoshidome, D. The importance of hydration thermodynamics in fragment-to-lead optimization. *ChemMedChem* **2014**, *9*, 2708−17.
(16) Kozakov, D.; Grove, L. E.; Hall, D. R.; Bohnuud, T.; Mottarella, S. E.; Luo, L.; Xia, B.; Beglov, D.; Vajda, S. The FTMap family of web servers for determining and characterizing ligand-binding hot spots of proteins. *Nat. Protoc.* **2015**, *10*, 733−755.
(17) Olsson, T. S. G.; Williams, M. A.; Pitt, W. R.; Ladbury, J. E. The thermodynamics of protein-ligand interaction and solvation: insights for ligand design. *J. Mol. Biol.* **2008**, *384*, 1002−17.
(18) Hendlich, M.; Rippmann, F.; Barnickel, G. LIGSITE: Automatic and efficient detection of potential small molecule-binding sites in proteins. *J. Mol. Graphics Modell.* **1997**, *15*, 359−363.
(19) Kawabata, T. Detection of multiscale pockets on protein surfaces using mathematical morphology. *Proteins: Struct., Funct., Genet.* **2010**, *78*, 1195−211.
(20) Cole, J. C. Onward development of GOLD: selective dockings using known protein properties. *EuroQSAR 2002: Des. Drugs Crop Protect: Processes, Problems, Solutions*; 2003; pp 140−143.
(21) Mysinger, M. M.; Carchia, M.; Irwin, J. J.; Shoichet, B. K. Directory of useful decoys, enhanced (DUD-E): Better ligands and decoys for better benchmarking. *J. Med. Chem.* **2012**, *55*, 6582−6594.
(22) Pagadala, N. S.; Syed, K.; Tuszynski, J. Software for molecular docking: a review. *Biophys. Rev.* **2017**, *9*, 91−102.
(23) Kruger, D. M.; Evers, A. Comparison of Structure- and Ligand-Based Virtual Screening Protocols Considering Hit List Complementarity and Enrichment Factors. *ChemMedChem* **2010**, *5*, 148−158.
(24) Roca, C.; Requena, C.; Sebastián-Pérez, V.; Malhotra, S.; Radoux, C.; Pérez, C.; Martinez, A.; Antonio Páez, J.; Blundell, T. L.; Campillo, N. E. Identification of new allosteric sites and modulators of AChE through computational and experimental tools. *J. Enzyme Inhib. Med. Chem.* **2018**, *33*, 1034−1047.
(25) Friesner, R. A.; Murphy, R. B.; Repasky, M. P.; Frye, L. L.; Greenwood, J. R.; Halgren, T. A.; Sanschagrin, P. C.; Mainz, D. T. Extra precision glide: docking and scoring incorporating a model of hydrophobic enclosure for protein-ligand complexes. *J. Med. Chem.* **2006**, *49*, 6177−96.
(26) Radoux, C. J. The Automatic Detection of Small Molecule Binding Hotspots on Proteins Applying Hotspots to Structure-Based Drug Design. Ph.D. thesis, University of Cambridge, 2018.
(27) Truchon, J.-F.; Bayly, C. I. Evaluating Virtual Screening Methods: Good and Bad Metrics for the "Early Recognition" Problem. *J. Chem. Inf. Model.* **2007**, *47*, 488−508.

https://dx.doi.org/10.1021/acs.jcim.9b00996
J. Chem. Inf. Model. 2020, 60, 1911−1916